PCCP

Accepted Manuscript

ROYAL SOCIETY OF CHEMISTRY

www.rsc.org/pccp

Octahedral Aromaticity in $^{2S+1}A_{1g}$ X_6^q Clusters (X = Li–C and Be–Si, S = 0–3, and q = -2–+4)

Ouissam El Bakouri[a], Miquel Duran[a], Jordi Poater[b], Ferran Feixas*[,a] and Miquel Solà*[,a]

[a] *Institut de Química Computacional i Catàlisi (IQCC) and Departament de Química, Universitat de Girona, Campus Montilivi, 17071 Girona, Spain. E-mail: miquel.sola@udg.edu*

[b] *Department of Theoretical Chemistry and Amsterdam Center for Multiscale Modeling, Vrije Universiteit Amsterdam, De Boeleaan 1083, NL-1081HV Amsterdam, The Netherlands*

Abstract

It is generally observed that quintessential aromatic compounds have delocalised electronic configurations that are of closed-shell or open-shell half-filled with same spin electrons. Guided by this property, we search for aromatic octahedral clusters of the type X_6^q (X = Li–C and Be–Si, q = -2–+4) in $^{2S+1}A_{1g}$ electronic states with spin multiplicities ranging from singlet to septet. With some exceptions, we find that closed-shell or open-shell half-filled with same spin electrons systems have large multicentre indices and negative NICS values that are characteristic patterns of aromatic compounds. Our results confirm the existence of octahedral aromaticity but do not allow us to define a general rule for octahedral aromaticity because the ordering of molecular orbitals does not remain the same for different octahedral clusters.

Introduction

The synthesis of *closo* borohydride $B_{10}H_{10}^{2-}$ by Lipscomb[1, 2] in 1959 and the discovery in 1962 of the first derivatives of *closo*-dodecaborate and *closo*-decaborate by Muetterties's group[3, 4] expanded the concept of aromaticity from two to three dimensions. *Closo* borohydride clusters with a general formula of $[B_nH_n]^{2-}$ are quite stable boron clusters that have a polyhedron structure with triangular faces.[1] Their stability is at odds with most borane compounds that are electron-deficient compounds, highly reactive, and unstable. *Closo* borohydride clusters are aromatic systems that obey Wade's 2n+2 electron rule,[5, 6] where n is the number of vertexes of the polyhedron, or Mingos' rule that is 4n+2.[7, 8] Both rules are equivalent, since Wade's rule refers to the skeletal electrons (all valence electrons except those of the B–H bonds), whereas Mingos' rule incorporates also the exo electrons corresponding to the B–H bonds, thus referring to the total number of valence electrons. Although the meaning of n in the 4n+2 Mingos and Hückel rules is different, some of us recently showed a connection between classical aromatic hydrocarbons and *closo* borohydride clusters that provides a link between the classical π-aromaticity and three-dimensional (3D) aromaticity.[9] Another well-known example of 3D aromaticity is the so-called spherical aromaticity. It applies to molecules that possess a molecular structure close to an sphere.[10] Fullerenes are the most characteristic examples of spherical aromatic compounds.[11, 12] There are two rules of spherical aromaticity, namely, the $2(n+1)^2$ Hirsch's rule[13, 14] for closed-shell systems and the $2n^2+2n+1$ ($S = n + ½$) rule[15] for open-shell compounds. Both rules are based on the fact that the wavefunctions of a uniform electron gas surrounding the surface of an sphere are characterized by the angular momentum quantum number l (l = 0, 1, 2…) similar to the situation found for atomic orbitals. Each energy level is 2l+1 times degenerated, and, therefore, π-shells are completely filled when we have 2, 8, 18, 32, 50, 72… electrons, i.e., $2(n+1)^2$ electrons. Similarly, an aromatic situation with the degenerate HOMOs occupied with half-filled electrons in parallel spin with the rest of lower levels orbitals being full-filled is reached for a number of electrons equals to 1, 5, 13, 25, 41, 61, 75…, i.e., for spherical species with $2n^2+2n+1$ π-electrons and with an electronic spin of S = n + ½. For instance, C_{60}^{10+} and C_{80}^{8+} are aromatic according to the Hirsch rule, whereas C_{60}^{1-} (S = 11/2) and C_{70}^{5-} (S = 13/2) obey the $2n^2+2n+1$ (S = n + ½) rule and are also aromatic. Yu and coworkers have recently reported that oxide cluster Ce_6O_8 exhibits d-atomic orbital-based spherical σ aromaticity.[16] In 1987, the 1,3-dehydro-5,7-adamantanedyl dication was described by Schleyer et al.[17] as a 3D homoaromatic species. Recently, the cubic aromaticity has been described as a new form of 3D aromaticity[18] and the 6n + 2 rule was proposed for this type of 3D aromaticity.[18]

Few octahedral systems have been described as aromatic. To our knowledge only five cases have been reported, namely, the $B_6H_6^{2-}$ *closo* borane cluster,[19] the eight σ-electrons H_6^{2-} species,[20] and the metalloaromatic[21, 22] Be_6 in the quintet state[23] and the singlet Au_6^{2-} and Al_6^{2-} clusters.[24, 25] Experimentally, however, only the O_h $B_6H_6^{2-}$ and Al_6^{2-} clusters have been observed, the latter in the form of $LiAl_6^-$.[25] Interestingly, B_6^{2-} that is valence isoelectronic with Al_6^{2-} has a planar D_{2h} molecular structure and it is antiaromatic.[26, 27] Hyunh and Alexandrova studied the $B_{6-n}Al_n^{2-}$ (n = 0–6) systems and found that the planar structure of B_6^{2-} persists until n = 5.[28] M_6Li_2 (M = Cu, Ag, Au) with pseudo-O_h symmetry were also found aromatic.[29] It is worth noting that O_h Si_6^{2-}, which is valence isoelectronic with $B_6H_6^{2-}$, was found to be antiaromatic according to NICS(0) values.[19]

In all examples of known 3D aromaticity the systems described as aromatic have a closed-shell or a half-filled shell with same spin electrons structure. These two types of electronic structures seem to offer good prospects of aromaticity.[24] Thus, we have followed this recipe in the quest for aromatic species with octahedral symmetry. Our search includes all species of the type O_h X_6^q (X = Li–C and Be–Si) with charges going from -2 to +4 and in $^{2S+1}A_{1g}$ electronic states with spin multiplicities ranging from singlet (S = 0) to septet (S = 3). We have not included atoms from the groups 15 to 18 due to the little tendency of the atoms of these groups to form clusters. It is worth emphasizing that our aim is not to find the lowest lying isomer for the $^{2S+1}A_{1g}$ X_6^q species but to analyse octahedral species with two objectives. First, we want to check whether a closed-shell structure or a half-filled shell with same spin electrons in O_h species is a sufficient requirement to generate aromaticity and, second, we aim to investigate the existence of a possible rule of aromaticity for octahedral compounds analogous to the Wade-Mingos rule for *closo* borane compounds.

Methods

All geometry optimizations were performed with the Gaussian 09 package[30] by using the B3LYP[31-33] hybrid density functional and the 6-311++G(3df,3pd) basis set[34] without symmetry constraints. Analytical Hessians were computed to confirm that the optimized structures are indeed minima (zero imaginary frequencies). The unrestricted formalism was used for all open-shell calculations. Computed relative energies between electronic states and atomization energies contain zero point energy corrections (ZPE). Atomization energies were calculated with respect to the lowest in energy atomic fragments. Kohn–Sham orbitals and eigenvalues were calculated with the B3LYP functional. Although Kohn-Sham orbitals are mathematical constructs used to build the electron density in density functional theory, the validity of these orbitals is justified by the work of Baerends[35] and Hoffmann[36] who found that the shape, symmetry, and energetic order of the Kohn–Sham orbitals are very similar to those calculated with the Hartree-Fock method. Aromaticity was evaluated at the same level of theory by means of multicentre electron sharing indices (MCI),[37, 38] delocalisation indices (DIs),[39-41] and nucleus-independent chemical shift (NICS)[42] obtained using the GIAO approximation.[43] MCIs provide a measure of electron sharing among the atoms considered.[38] DIs are two-centre electron sharing indices (i.e., two-centre MCIs) that measure electron sharing between two atoms.[39-41] Although several partitions can be used to define the atomic regions needed to calculate DIs and MCIs, we made use of the molecular partition based on the fuzzy atom approach[44] because of the presence of non-nuclear attractors in some of the species considered as revealed by the quantum theory of the atoms in molecules (QTAIM).[45, 46] It was shown that for bonds with a reduced polarization such as all bonds analysed here, the fuzzy atom approach and QTAIM yield quite similar results.[47] The atomic regions based on the fuzzy atom approach were defined with the APOST-3D program.[48] The MCI and DI indices were obtained with the ESI-3D program.[49, 50] To gain further insight into the aromaticity of O_h $^1A_{1g}$ X_6^q clusters, the individual canonical molecular orbital (CMO) contributions[51, 52] to the overall NICS value of closed shell species were computed with the NBO 6.0 program.[53] Finally, let us note that NICS calculations for open-shell systems are approximate since they contain only the contributions arising from the perturbation of the wavefunction due to the external magnetic field.[54, 55]

Results and discussion

Combination of the four valence *ns* and *np* atomic orbitals of atom X in an O_h $^{2S+1}A_{1g}$ X_6^q species leads to twenty-four molecular orbitals. Figure 1 depicts the sixteen lowest-lying molecular orbitals (MOs) present in O_h $^{2S+1}A_{1g}$ X_6^q clusters. The same MOs with the same shape and energetic ordering were reported by Schleyer et al. for O_h Si_6^{2-}.[19] From these orbitals, one could propose the series 2, 8, 12, 14, 20, 26, 32… as the magic numbers that lead to closed-shell aromatic species. For open-shell clusters, the magic numbers would be 1, 5, 10, 13, 17, 23, 29… Unfortunately, these series of magic numbers cannot be generalized because the energetic order of the MOs shown in Figure 1 changes depending on the X atoms and the multiplicity and the charge of the O_h $^{2S+1}A_{1g}$ X_6^q clusters. As Figure S1 in the SI shows, the $2a_{1g}$ and $1t_{2g}$ MOs always become more stable than the $1e_g$ ones for the clusters of the second period (X = Li, Be and B). Moreover, in some clusters the $2a_{1g}$ are more stable than the $1t_{2g}$ and in other cases is the other way round. Basically, the energy difference between $1e_g$, the radial $2a_{1g}$, and the tangential $1t_{2g}$ is small and the ordering of the different orbitals changes from one cluster to another. This leads to the first conclusion of this work: it is not possible to derive a general rule for octahedral aromaticity similar to those of spherical aromaticity. Interestingly, however, the first two shells ($1a_{1g}$ and $1t_{1u}$) are always the same for all clusters analysed. Therefore, for small number of valence electrons, the magic numbers 2 and 8 (closed-shell) or 1 and 5 (open-shell) for octahedral aromaticity hold and they are the same as those found in spherical and cubic aromatic species.

FIGURE 1, here

Nevertheless, we decided to look for octahedral aromatic species by generating clusters with closed shells or half-filled shells with same spin electrons. To this end, we constructed all clusters with formula X_6^q (X = Li–C and Be–Si) having $^{2S+1}A_{1g}$ electronic states and with charges going from -2 to +4 and spin multiplicities ranging from singlet to septet (S=0, ½, 1…3). Table 1 gathers all clusters with a combination of charge and spin that i) lead to electronic closed shell or half-filled shell with same spin electrons configurations and ii) are minima in the potential energy surface. For instance, for $^{2S+1}A_{1g}$ C_6^q, all clusters found with octahedral symmetry are n-order saddle points. All O_h $^{2S+1}A_{1g}$ X_6^q clusters that are stationary points with imaginary frequencies are collected in Table S5 of the SI. As a whole, we found twenty-three O_h $^{2S+1}A_{1g}$ X_6^q clusters that are minima but not necessarily the global minimum. Moreover, three out of these twenty-three minima have a negative energy of atomization (Table 1). These clusters are metastable, i.e., the system is energetically stabilized by dissociation into atomic fragments in their lowest-lying states but with a Coulombic barrier for the dissociation, as found for instance in the N_2^{2+} compound[56, 57] or in the dissociation of Ge_4^{2+}into two Ge_2^+ fragments.[58]

As can be seen in Table 1, the X–X bond distance generally increases from the second to the third period X atoms and for the same period decreases in the order group 1 > group 2 > group 13 > group 15. Not unexpectedly, the X–X bond distance decreases following the same tendency of the atomic radius of X atoms. In addition, the large bond distances of alkalimetals can be attributed to the low number of valence electrons that occupy the lowest-lying bonding orbitals that leads to structures with relatively low dissociation energies. This is the case of Li_6^+ in the $^4A_{1g}$ state that has five valence electrons fully occupying the $1a_{1g}$ orbital and half filling the degenerate $1t_{1u}$ orbitals. This cluster has a dissociation energy to 5Li + Li^+ of only 123.5 kcal/mol.

TABLE 1, here

The lack of all-metal and semimetal aromatic clusters that can serve as reference systems (like benzene does in classical aromatic organic molecules) makes the measure of aromaticity in these systems difficult.[22, 59] Indeed, most of the current available methods to quantify aromaticity have been designed to measure the aromaticity of organic 2D molecules and take benzene or other aromatic organic molecules as a reference in their definitions. Moreover, computation of energetic-based indicators such as resonance energies (RE) or aromatic stabilization energies (ASE)[60] is challenging for these clusters also because of the lack of appropriate reference systems.[61, 62] For this reason, MCI and NICS are probably to date the most suitable indicators of metalloaromaticity.[63] In Table 1 we have gathered the multicentre index involving the six X atoms of the octahedron (MCI_6), of four equatorial X atoms (MCI_4), and of three X atoms in the face of the octahedron (MCI_3). We have also computed the NICS in the centre of the octahedron ($NICS(0)_6$) and in the centre of an octahedron face ($NICS(0)_3$).

Finally, we have collected the so-called *para*-delocalisation indices (PDI) that are the DIs between opposed axial atoms in the octahedron. This index is analogous to the PDI used as a measure of aromaticity in six-membered rings of polycyclic aromatic hydrocarbons.[64, 65]

Among all systems gathered in Table 1, the aromaticity of $^{1}A_{1g}$ Al_6^{2-} was studied previously and it has been concluded that this cluster is aromatic.[25, 28] The relatively large MCI_6, MCI_4, MCI_3, and PDI values and the negative $NICS(0)_6$ and $NICS(0)_3$ provide further support to the aromatic character of this cluster. Values of the different indices of this system are used as a reference to discuss the rest of the series. Interestingly, $^{1}A_{1g}$ Al_6^{2-} has the largest MCI_4 and the most negative $NICS(0)_6$ and $NICS(0)_3$ values. The CMO-NICS contributions collected in Figure 2a show that all occupied orbitals of Al_6^{2-} exhibit strong diamagnetic character. On the other hand, the largest PDI and MCI_3 correspond to $^{1}A_{1g}$ B_6^{2+}, whereas the system with the highest MCI_6 is Be_6^{2+}. Linear correlations between the different indices analysed, which are given in Table S3, indicate that in most cases correlations are rather poor. The best linear correlations among different indices are $NICS(0)_6$-$NICS(0)_3$ (r^2=0.88), PDI-MCI_3 (r^2=0.82), $NICS(0)_6$-MCI_4 (r^2=0.71) and $NICS(0)_3$-MCI_4 (r^2=0.66). Somewhat surprisingly from the fact that usually the MCI is lower when the number of atoms involved in the measure increases, in most cases MCI_6 of $^{2S+1}A_{1g}$ X_6^{q} clusters in Table 1 are greater than MCI_4. On the contrary, as expected, PDI is always larger than MCI_3 and this index in turn is larger than MCI_4. If we assume that systems with relatively large electronics indices (MCI_6 > 0.02; MCI_4 > 0.02; MCI_3 > 0.05, and PDI>0.20) and negative $NICS(0)_6$ and $NICS(0)_3$ values are aromatic, then sixteen out of twenty three species are aromatic, $^{1}A_{1g}$ Mg_6 is antiaromatic, and the six clusters left are in the border between aromatic and antiaromatic species and we can classify them as non-aromatic. Therefore, we can conclude that in general, but not always, closed-shell or a half-filled shell with same spin electrons electronic configurations in octahedral species lead to aromatic clusters. It is worth noting that, as Table 1 shows, all second period octahedral compounds (eg. Li, Be, and B) are aromatic while nonaromatic and antiaromatic species are only observed for compounds formed by elements of the third period. Let us finally discuss in more detail the five following clusters that deserve further comments: Li_6^+, Be_6, Mg_6, Al_6^{2-}, and Si_6^{2-}.

Li_6^+ has two possible electronic configurations with half-filled shells with same spin electrons, namely, $1a_{1g}^2 1t_{1u}^3$ (S = 3/2, $^4A_{1g}$) and $1a_{1g}^1 1t_{1u}^3 2a_{1g}^1$ (S = 5/2, $^6A_{1g}$) with atomization energies of 123.5 and 61.2 kcal/mol, respectively. The energy difference between these two electronic states is 62.3 kcal/mol, the $^4A_{1g}$ being the most stable. In these states, the X–X distance and the aromaticity parameters are similar. From the aromatic indicators of Table 1, one can classify these clusters as moderately aromatic. Neither $^4A_{1g}$ nor $^6A_{1g}$ of octahedral Li_6^+ is the ground state for this cluster. Indeed, the most stable isomer for Li_6^+ at the CCSD(T)/cc-pCVDZ level has a C_{2v} structure and an atomization energy of 142.6 kcal/mol (23.8 kcal/mol per atom).[66] This C_{2v} structure with S = ½ is not aromatic at all (MCI_6 = 0.006 e; $NICS(0)_6$ = 44.70 ppm; PDI = 0.241 e at B3LYP/6-311G++(3df,3pd)).

The electronic state of the octahedral Be_6 cluster is $^5A_{1g}$. Aromaticity descriptors in Table 1 denote a clear aromatic character for this species. The presence of twelve valence electrons instead of five in $^4A_{1g}$ Li_6^+ makes the Be–Be bond stronger (atomization energy is 156.9 kcal/mol) and the Be–Be distance shorter

(2.040 Å). The electron configuration is $1a_{1g}^2 1t_{1u}^6 2a_{1g}^1 1t_{2g}^3$, the highest-lying four valence electrons being same spin electrons half-filling the $2a_{1g}$ and $1t_{2g}$ MOs. Like for $^4A_{1g}$ Li_6^+, the $^5A_{1g}$ Be_6 state is an excited state for Be_6, although this conclusion depends on the level of calculation. Indeed, Be_6 is the first Be cluster the ground state of whom is controversial[67, 68] and for some methods the O_h $^5A_{1g}$ is the ground state.[23] Different authors have pointed out the following ground states: O_h $^5A_{1g}$,[23] D_{3d} $^3A_{1g}$,[69, 70] C_{2v} $^1A_1$,[69] C_{2h} ^3A_u,[26] and D_{2h} ^1A_g.[67, 69] All CCSD calculations favour the D_{2h} ^1A_g state.[67, 69] In this most stable D_{2h} ^1A_g electronic state the cluster can be considered non-aromatic (MCI_6 = 0.089 e; $NICS(0)_6$ = 3.72 ppm; PDI = 0.532 e at B3LYP/6-311G++(3df,3pd)).

$^1A_{1g}$ Mg_6 is a particular case for its long X–X distance (3.702 Å). The electronic configuration is $1a_{1g}^2 1t_{1u}^6 e_g^4$. Its positive NICS and low values of electronic indices indicate antiaromatic character. CMO-NICS results of Figure S2 show that the antiaromatic character is mainly due to the contribution from $1e_g$ orbitals. The lack of aromaticity in this octahedral closed-shell $^1A_{1g}$ Mg_6 species is somewhat surprising and the reasons for this unexpected behaviour are unclear. However, there are other examples of similar situations. For instance, borazine has an electronic structure similar to benzene and should be aromatic according to Hückel's rule but it is not.[71-73]

Al_6^{2-} has two possible electronic configurations. One that is closed-shell, $1a_{1g}^2 1t_{1u}^6 1e_g^4 2a_{1g}^2 1t_{2g}^6$ (S = 0, $^1A_{1g}$), and another one with two half-filled shells with same spin electrons, $1a_{1g}^2 1t_{1u}^6 1e_g^4 2a_{1g}^2 1t_{2g}^3 2t_{1u}^3$ (S = 3, $^7A_{1g}$). The energy difference between these two electronic states is 44.7 kcal/mol. The $^1A_{1g}$ Al_6^{2-} cluster was studied previously and it was concluded that this cluster is aromatic.[25, 28] Our indicators also support this conclusion. On the other hand, the

$^{7}A_{1g}$ Al_6^{2-} cluster with positive NICS and low electron sharing indices is classified as non-aromatic. It is worth noting that, with the exception of Mg_6^{2-}, closed-shell electronic structures ($^{1}A_{1g}$) are found to be more aromatic than open-shell ones.

For the $^{1}A_{1g}$ Si_6^{2-} cluster, the octahedral geometry is the most stable.[74] This cluster was detected experimentally in time-of-flight mass spectra as Si_6Na_2.[75] As said in the introduction octahedral $^{1}A_{1g}$ Si_6^{2-} cluster with electronic configuration $1a_{1g}^{2}1t_{1u}^{6}1e_{g}^{4}2a_{1g}^{2}1t_{2g}^{6}2t_{1u}^{6}$ was found to be antiaromatic according to $NICS(0)_6$ values.[19] We also obtain positive $NICS(0)_6$ values, although $NICS(0)_3$ are negative. CMO-NICS contributions to $NICS(0)_6$ of Figure 2b show that positive values come from the filled $2t_{1u}$ MOs.[19, 76] This situation resembles that of the $Al_3H_3^{2-}$ cluster in which the tangential orbitals contribute with positive CMO-NICS to the total NICS(0) value.[77, 78] The negative $NICS(0)_3$ value in the $^{1}A_{1g}$ Si_6^{2-} cluster appears due to an important reduction of the antiaromatic character of the $2t_{1u}$ orbitals when calculated in the face of the octahedron. The computed MCI_6 and MCI_4 for $^{1}A_{1g}$ Si_6^{2-} are not particularly large but not negligible either. MCI_3 gives a significantly large value which is line with the negative $NICS(0)_3$ value. These results could indicate a certain degree of electron delocalisation among the atoms that form the faces of the octahedron but this electron sharing is not extended among the six atoms of the system. As a whole, we classify this system in the border between aromatic and antiaromatic clusters, i.e., as a non-aromatic species.

Conclusions

From the present study we can derive the following conclusions. First, generally but not always closed-shell or open-shell half-filled with same spin electrons electronic configurations in octahedral symmetry have aromatic character with large electron sharing indices and negative NICS values. Therefore, an electronic configuration with a closed-shell or an open-shell half-filled with same spin electrons is not a sufficient condition for aromaticity, although it seems to help. Second, our study confirms the existence of fifteen new clusters (Al_6^{2-} was already known) that have octahedral aromaticity. And finally, despite our results support the existence of octahedral aromaticity they do not allow us to propose a rule for octahedral aromaticity equivalent to the $2(n+1)^2$ Hirsch's rule for spherical aromaticity because the ordering of molecular orbitals does not remain the same for different octahedral clusters.

Acknowledgements

This work has been supported by the Ministerio de Economía y Competitividad (MINECO) of Spain (Project CTQ2014-54306-P) and the Generalitat de Catalunya (project 2014SGR931, Xarxa de Referència en Química Teòrica i Computacional, ICREA Academia 2014 prize for M.S., and grant No. 2014FI_B 00429 to O.E.B.). F.F. acknowledges financial support of the Beatriu de Pinós programme from AGAUR for the postdoctoral grants BP_A_00339 and BP_A2_00022. The EU under the FEDER grant UNGI10-4E-801 (European Fund for Regional Development) has also funded this research. J. P. thanks the National Research School Combination - Catalysis (NRSC-C), and The Netherlands Organization for Scientific Research (NWO/CW and NWO/NCF).

Keywords: octahedral compounds · electronic structure · metallic bonding · aromaticity · multicentre indices · nucleus independent chemical shifts

Supplementary Information

Cartesian coordinates of all stationary points located. The molecular orbital distribution for all species studied. The CMO-NICS values for all clusters in $^1A_{1g}$ electronic states.

References

1. W. N. Lipscomb, *Boron Hydrides*, W. A. Benjamin, New York, 1963.
2. W. N. Lipscomb, A. R. Pitochelli and M. F. Hawthorne, *J. Am. Chem. Soc.*, 1959, **81**, 5833-5834.
3. F. Klanberg, D. R. Eaton, L. J. Guggenberger and E. L. Muetterties, *Inorg. Chem.*, 1967, **6**, 1271-1281.
4. W. H. Knoth, H. C. Miller, D. C. England, G. W. Parshall and E. L. Muetterties, *J. Am. Chem. Soc.*, 1962, **84**, 1056-1057.
5. K. Wade, *J. Chem. Soc. D: Chem. Commun.*, 1971, 792-793.
6. K. Wade, *Electron-deficient Compounds*, Nelson and Sons, Ltd., London, 1971.
7. D. M. P. Mingos, *Nature Phys. Sci.*, 1972, **236**, 99-102.
8. D. M. P. Mingos, *Acc. Chem. Res.*, 1984, **17**, 311-319.
9. J. Poater, M. Solà, C. Viñas and F. Teixidor, *Angew. Chem. Int. Ed.*, 2014, **53**, 12191–12195.
10. Z. F. Chen and R. King, *Chem. Rev.*, 2005, **105**, 3613-3642.
11. M. Bühl and A. Hirsch, *Chem. Rev.*, 2001, **101**, 1153-1183.
12. A. Sanz Matias, R. W. A. Havenith, M. Alcami and A. Ceulemans, *Phys. Chem. Chem. Phys.*, 2015, DOI: 10.1039/C5CP04970A.
13. Z. Chen, H. Jiao, A. Hirsch and W. Thiel, *J. Mol. Model.*, 2001, **7**, 161-163.
14. A. Hirsch, Z. Chen and H. Jiao, *Angew. Chem. Int. Ed.*, 2000, **39**, 3915-3917.
15. J. Poater and M. Solà, *Chem. Commun.*, 2011, **47**, 11647-11649.
16. X. Yu, A. R. Oganov, I. A. Popov and A. I. Boldyrev, *J. Comput. Chem.*, 2016, **37**, 103-109.
17. M. Bremer, P. von Ragué Schleyer, K. Schötz, M. Kausch and M. Schindler, *Angew. Chem. Int. Ed. Engl.*, 1987, **26**, 761-763.
18. P. Cui, H.-S. Hu, B. Zhao, J. T. Miller, P. Cheng and J. Li, *Nat. Commun.*, 2015, **6**, 6331.
19. R. B. King, T. Heine, C. Corminboeuf and P. v. R. Schleyer, *J. Am. Chem. Soc.*, 2004, **126**, 430-431.
20. H. Jiao, P. v. R. Schleyer and M. N. Glukhovtsev, *J. Phys. Chem.*, 1996, **100**, 12299-12304.
21. A. I. Boldyrev and L.-S. Wang, *Chem. Rev.*, 2005, **105**, 3716-3757.
22. F. Feixas, E. Matito, J. Poater and M. Solà, *WIREs Comput. Mol. Sci.*, 2013, **3**, 105-122.
23. S. Srinivas and J. Jellinek, *J. Chem. Phys.*, 2004, **121**, 7243-7252.
24. Z. Chen, S. Neukermans, X. Wang, E. Janssens, Z. Zhou, R. E. Silverans, R. B. King, P. v. R. Schleyer and P. Lievens, *J. Am. Chem. Soc.*, 2006, **128**, 12829-12834.
25. A. E. Kuznetsov, A. I. Boldyrev, H.-J. Zhai, X. Li and L.-S. Wang, *J. Am. Chem. Soc.*, 2002, **124**, 11791-11801.

26. A. N. Alexandrova, A. I. Boldyrev, H.-J. Zhai, L.-S. Wang, E. Steiner and P. W. Fowler, *J. Phys. Chem. A*, 2003, **107**, 1359-1369.
27. J. Ma, Z. Li, K. Fan and M. Zhou, *Chem. Phys. Lett.*, 2003, **372**, 708-716.
28. M. T. Huynh and A. N. Alexandrova, *J. Phys. Chem. Lett.*, 2011, **2**, 2046-2051.
29. C. Corminboeuf, C. S. Wannere, D. Roy, R. B. King and P. v. R. Schleyer, *Inorg. Chem*, 2006, **45**, 214-219.
30. M. J. Frisch, G. W. Trucks, H. B. Schlegel, G. E. Scuseria, M. A. Robb, J. R. Cheeseman, G. Scalmani, V. Barone, B. Mennucci, G. A. Petersson, H. Nakatsuji, M. Caricato, X. Li, H. P. Hratchian, A. F. Izmaylov, J. Bloino, G. Zheng, J. L. Sonnenberg, M. Hada, M. Ehara, K. Toyota, R. Fukuda, J. Hasegawa, M. Ishida, T. Nakajima, Y. Honda, O. Kitao, H. Nakai, T. Vreven, J. A. Montgomery Jr., J. E. Peralta, F. Ogliaro, M. Bearpark, J. J. Heyd, E. Brothers, K. N. Kudin, V. N. Staroverov, R. Kobayashi, J. Normand, K. Raghavachari, A. Rendell, J. C. Burant, S. S. Iyengar, J. Tomasi, M. Cossi, N. Rega, J. M. Millam, M. Klene, J. E. Knox, J. B. Cross, V. Bakken, C. Adamo, J. Jaramillo, R. Gomperts, R. E. Stratmann, O. Yazyev, A. J. Austin, R. Cammi, C. Pomelli, J. W. Ochterski, R. L. Martin, K. Morokuma, V. G. Zakrzewski, G. A. Voth, P. Salvador, J. J. Dannenberg, S. Dapprich, A. D. Daniels, Ö. Farkas, J. B. Foresman, J. V. Ortiz, J. Cioslowski and D. J. Fox, *Journal*, 2009.
31. A. D. Becke, *J. Chem. Phys.*, 1993, **98**, 5648-5652.
32. C. Lee, W. Yang and R. G. Parr, *Phys. Rev. B*, 1988, **37**, 785-789.
33. P. J. Stephens, F. J. Devlin, C. F. Chabalowski and M. J. Frisch, *J. Phys. Chem.*, 1994, **98**, 11623-11627.
34. M. J. Frisch, J. A. Pople and J. S. Binkley, *J. Chem. Phys.*, 1984, **80**, 3265-3269.
35. E. J. Baerends and O. V. Gritsenko, *J. Phys. Chem. A*, 1997, **101**, 5383-5403.
36. R. Stowasser and R. Hoffmann, *J. Am. Chem. Soc.*, 1999, **121**, 3414-3420.
37. P. Bultinck, R. Ponec and S. Van Damme, *J. Phys. Org. Chem.*, 2005, **18**, 706-718.
38. F. Feixas, E. Matito, J. Poater and M. Solà, *Chem. Soc. Rev.*, 2015, **44**, 6434–6451.
39. R. F. W. Bader and M. E. Stephens, *J. Am. Chem. Soc.*, 1975, **97**, 7391-7399.
40. X. Fradera, M. A. Austen and R. F. W. Bader, *J. Phys. Chem. A*, 1999, **103**, 304-314.
41. X. Fradera, J. Poater, S. Simon, M. Duran and M. Solà, *Theor. Chem. Acc.*, 2002, **108**, 214-224.
42. P. v. R. Schleyer, C. Maerker, A. Dransfeld, H. Jiao and N. J. R. van Eikema Hommes, *J. Am. Chem. Soc.*, 1996, **118**, 6317-6318.
43. K. Wolinski, J. F. Hilton and P. Pulay, *J. Am. Chem. Soc.*, 1990, **112**, 8251-8260.
44. I. Mayer and P. Salvador, *Chem. Phys. Lett.*, 2004, **383**, 368-375.
45. R. F. W. Bader, *Atoms in Molecules: A Quantum Theory*, Clarendon, Oxford, 1990.
46. R. F. W. Bader, *Chem. Rev.*, 1991, **91**, 893-928.
47. E. Matito, J. Poater, M. Solà, M. Duran and P. Salvador, *J. Phys. Chem. A*, 2005, **109**, 9904-9910.
48. P. Salvador and E. Ramos-Cordoba, *APOST-3D*, Institute of Computational Chemistry and Catalysis, University of Girona, Girona, 2014.

49. E. Matito, M. Duran and M. Solà, *J. Chem. Phys.*, 2005, **122**, 014109.
50. E. Matito, *ESI-3D: Electron Sharing Indexes Program for 3D Molecular Space Partitioning*, http://iqc.udg.es/~eduard/ESI, Institute of Computational Chemistry and Catalysis, Girona, 2006.
51. T. Heine, P. v. R. Schleyer, C. Corminboeuf, G. Seifert, R. Reviakine and J. Weber, *J. Phys. Chem. A*, 2003, **107**, 6470-6475.
52. C. Corminboeuf, T. Heine, G. Seifert, P. v. R. Schleyer and J. Weber, *Phys. Chem. Chem. Phys.*, 2004, **6**, 273-276.
53. E. D. Glendening, J. K. Badenhoop, A. E. Reed, J. E. Carpenter, J. A. Bohmann, C. M. Morales, C. R. Landis and F. Weinhold, *NBO 6.0 program,* Theoretical Chemistry Institute and Department of Chemistry, University of Wisconsin, Madison, Wisconsin, 2013.
54. V. Gogonea, P. v. R. Schleyer and P. R. Schreiner, *Angew. Chem. Int. Ed.*, 1998, **37**, 1945-1948.
55. P. B. Karadakov, *J. Phys. Chem. A*, 2008, **112**, 7303-7309.
56. A. K. Edwards and R. M. Wood, *J. Chem. Phys.*, 1982, **76**, 2938-2942.
57. R. W. Wetmore and R. K. Boyd, *J. Phys. Chem.*, 1986, **90**, 5540-5551.
58. E. Díaz-Cervantes, J. Poater, J. Robles, M. Swart and M. Solà, *J. Phys. Chem. A*, 2013, **117**, 10462-10469.
59. F. Feixas, E. Matito, M. Duran, J. Poater and M. Solà, *Theor. Chem. Acc.*, 2011, **128**, 419-431.
60. M. K. Cyrański, *Chem. Rev.*, 2005, **105**, 3773-3811.
61. C.-G. Zhan, F. Zheng and D. A. Dixon, *J. Am. Chem. Soc.*, 2002, **124**, 14795-14803.
62. A. I. Boldyrev and A. E. Kuznetsov, *Inorg. Chem.*, 2002, **41**, 532-537.
63. F. Feixas, J. O. C. Jiménez-Halla, E. Matito, J. Poater and M. Solà, *J. Chem. Theory Comput.*, 2010, **6**, 1118–1130.
64. J. Poater, X. Fradera, M. Duran and M. Solà, *Chem. Eur. J.*, 2003, **9**, 400-406.
65. J. Poater, X. Fradera, M. Duran and M. Solà, *Chem. Eur. J.*, 2003, **9**, 1113-1122.
66. B. Temelso and C. D. Sherrill, *J. Chem. Phys.*, 2005, **122**, 064315.
67. Š. Martin, L. Daniel, K. Martin, P. Michal, Č. Ivan and N. Pavel, *J. Phys. B*, 2012, **45**, 085102.
68. M. C. Heaven, J. M. Merritt and V. E. Bondybey, *Ann. Rev. Phys. Chem.*, 2011, **62**, 375-393.
69. Y. Zhao, N. Li, W. G. Xu and Q. S. Li, *Int. J. Quantum Chem.*, 2007, **107**, 81-91.
70. M. K. Beyer, L. A. Kaledin, A. L. Kaledin, M. C. Heaven and V. E. Bondybey, *Chem. Phys.*, 2000, **262**, 15-23.
71. E. Maslowsky Jr., *Coord. Chem. Rev.*, 2011, **255**, 2746-2763.
72. R. Islas, E. Chamorro, J. Robles, T. Heine, J. Santos and G. Merino, *Struct. Chem.*, 2007, **18**, 833-839.
73. N. D. Charistos, A. G. Papadopoulos and M. P. Sigalas, *J. Phys. Chem. A*, 2014, **118**, 1113-1122.
74. M. Takahashi and Y. Kawazoe, *Chem. Phys. Lett.*, 2006, **418**, 475-480.
75. R. Kishi, S. Iwata, A. Nakajima and K. Kaya, *J. Chem. Phys.*, 1997, **107**, 3056-3070.
76. C. Corminboeuf, R. B. King and P. v. R. Schleyer, *ChemPhysChem*, 2007, **8**, 391-398.

77. J. M. Mercero, M. Piris, J. M. Matxain, X. Lopez and J. M. Ugalde, *J. Am. Chem. Soc.*, 2009, **131**, 6949-6951.
78. J. M. Mercero, A. I. Boldyrev, G. Merino and J. M. Ugalde, *Chem. Soc. Rev.*, 2015, **44**, 6519-6534.

Table 1 Molecular structures of octahedral clusters ${}^{2S+1}A_{1g}\,X_6^q$ that are minima on the potential surface. Values of X–X bond distance in Å, MCI and PDI in electrons, NICS in ppm, and ΔE_{atom} in kcal/mol. ΔE_{atom} is the atomization energy of cluster to the most stable atomic fragments.[a]

System	*q*	*Spin*	Electronic state	d(X–X)	MCI_6	MCI_4	MCI_3	$NICS(0)_6$	$NICS(0)_3$	PDI	ΔE_{atom}
Li_6	*1*	S=3/2	${}^4A_{1g}$	3.007	0.068	0.038	0.078	-19.17	-14.07	0.260	123.5
		S=5/2	${}^6A_{1g}$	3.112	0.069	0.035	0.077	-18.63	-13.72	0.258	61.2
Be_6	*-2*	S=3	${}^7A_{1g}$	2.129	0.061	0.055	0.137	-58.66	-45.88	0.584	130.1
	-1	S=3/2	${}^4A_{1g}$	2.050	0.121	0.066	0.175	-35.72	-17.16	0.656	205.9
	0	S=2	${}^5A_{1g}$	2.040	0.080	0.054	0.158	-31.54	-15.38	0.603	156.9
	2	S=0	${}^1A_{1g}$	2.135	0.140	0.068	0.158	-50.45	-37.13	0.521	136.5
	3	S=1/2	${}^2A_{1g}$	2.267	0.097	0.054	0.136	-43.21	-33.00	0.461	-25.2
B_6	*0*	S=1	${}^3A_{1g}$	1.675	0.085	0.060	0.174	-72.97	-53.40	0.769	488.8
	2	S=0	${}^1A_{1g}$	1.628	0.109	0.063	0.196	-47.64	-24.90	0.800	381.3
	3	S=1/2	${}^2A_{1g}$	1.677	0.072	0.039	0.175	-36.67	-19.02	0.742	59.8
	4	S=0	${}^1A_{1g}$	1.745	0.035	0.015	0.152	-22.98	-10.93	0.682	-37.3
Na_6	*-2*	S=0	${}^1A_{1g}$	3.605	0.022	0.035	0.078	-17.79	-16.99	0.330	41.4
		S=3	${}^7A_{1g}$	3.890	0.064	0.032	0.054	4.50	6.74	0.236	0.9
	1	S=3/2	${}^4A_{1g}$	3.602	0.061	0.038	0.064	-20.12	-15.64	0.237	100.1
Mg_6	*-2*	S=0	${}^1A_{1g}$	3.439	0.056	0.029	0.071	14.48	17.04	0.367	14.8
		S=3	${}^7A_{1g}$	3.096	0.057	0.063	0.105	-52.10	-44.09	0.511	-20.4
	0	S=0	${}^1A_{1g}$	3.702	0.001	0.003	0.031	10.99	10.53	0.286	12.6
	2	S=1	${}^3A_{1g}$	3.411	0.017	0.022	0.060	-3.11	-0.30	0.329	40.05
Al_6	*-2*	S=0	${}^1A_{1g}$	2.710	0.081	0.087	0.125	-80.73	-68.12	0.678	250.0
		S=3	${}^7A_{1g}$	2.865	0.038	0.030	0.120	15.74	8.61	0.573	205.3
	2	S=2	${}^5A_{1g}$	2.948	0.046	0.049	0.078	-24.86	-18.88	0.491	106.6
Si_6	*-2*	S=0	${}^1A_{1g}$	2.485	0.023	0.030	0.165	10.08	-14.73	0.772	527.0
	1	S=3/2	${}^4A_{1g}$	2.461	0.055	0.054	0.146	-43.57	-48.33	0.726	565.8

---

[a] For instance, in Mg_6^{2+} we have considered the atomization into 5Mg + Mg^{2+} rather than to 4Mg + $2Mg^+$ because the former has a lower energy.

Figure 1. Schematic molecular orbital energy levels for a typical octahedral cluster.

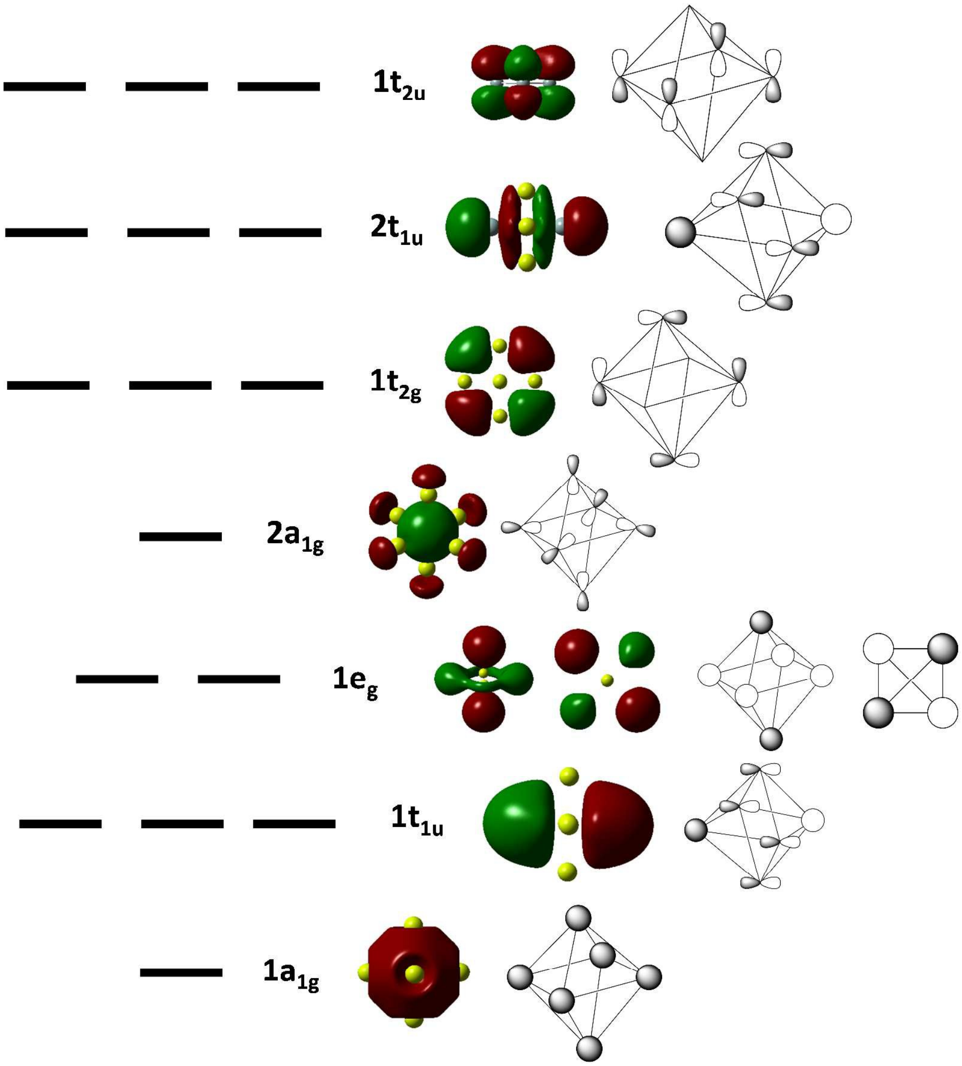

Figure 2. CMO-NICS$_6$(0) decomposition for (a) Al_6^{2-} and (b) Si_6^{2-} in their $^1A_{1g}$ electronic states.

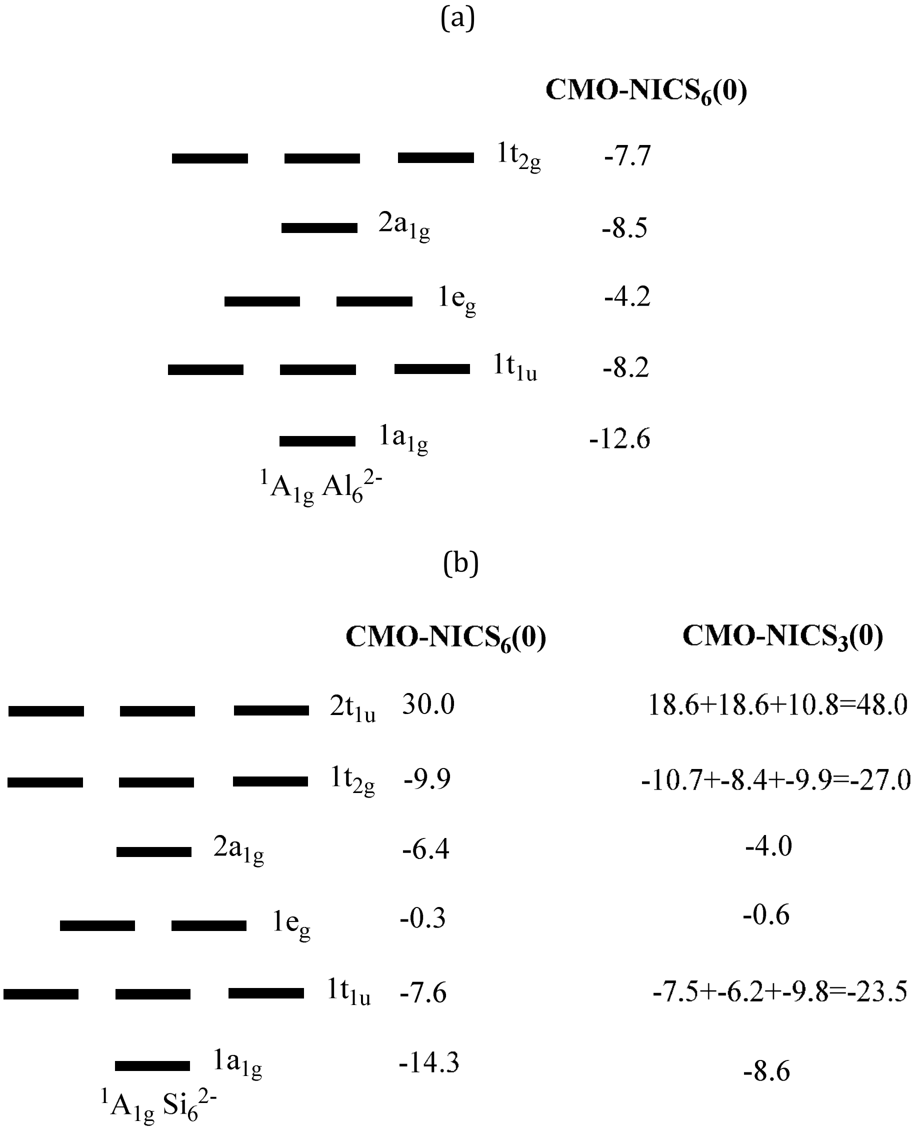

TABLE OF CONTENTS GRAPHIC

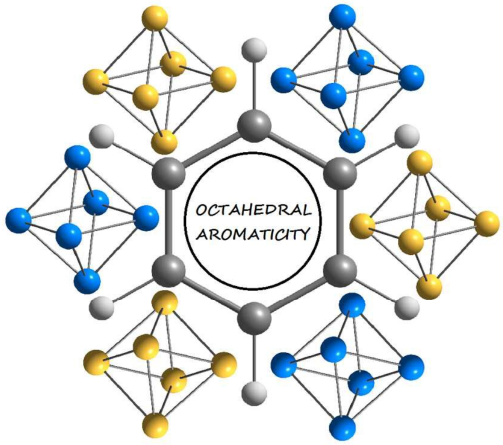

Octahedral aromaticity was found in most clusters of formula X_6^q (X = Li–C and Be–Si) with q = -2 to +4 and spin states ranging from singlet to septet that have electronic configurations of closed-shell or open half-filled shells with same spin electrons.